

**University of Massachusetts Amherst**

---

**From the Selected Works of Ashwin Ramasubramaniam**

---

November, 2010

# Tunable band gaps in bilayer graphene-BN heterostructures

Ashwin Ramasubramaniam, *University of Massachusetts - Amherst*

Doron Naveh

ELias Towe



Available at: [https://works.bepress.com/ashwin\\_ramasubramaniam/6/](https://works.bepress.com/ashwin_ramasubramaniam/6/)

# Tunable Band Gaps in Bilayer Graphene-BN Heterostructures

Ashwin Ramasubramanian\*

*Department of Mechanical and Industrial Engineering,  
University of Massachusetts Amherst, Amherst MA 01003*

Doron Naveh<sup>†</sup> and Elias Towe<sup>‡</sup>

*Department of Electrical and Computer Engineering,  
Carnegie Mellon University, Pittsburg PA 15213*

(Dated: November 11, 2010)

## Abstract

We investigate band-gap tuning of bilayer graphene between hexagonal boron nitride sheets, by external electric fields. Using density functional theory, we show that the gap is continuously tunable from 0 to 0.2 eV, and is robust to stacking disorder. Moreover, boron nitride sheets do not alter the fundamental response from that of free-standing bilayer graphene, apart from additional screening. The calculations suggest that the graphene-boron nitride heterostructures could provide a viable route to graphene-based electronic devices.

## I. INTRODUCTION

The nature and type of substrate on which graphene is supported critically influences the properties and characteristics of any electronic device fabricated from it. It is generally found, for example, that commonly used  $\text{SiO}_2$  substrates degrade the properties of pristine graphene, resulting in significantly compromised electron transport and device characteristics.<sup>1-5</sup> While the use of freely suspended graphene shows superior transport properties and impressive device characteristics, this form of graphene imposes several obstacles to device fabrication. It is therefore important to explore other substrates for supporting graphene. Recently, hexagonal boron nitride (hBN) has emerged as a potentially suitable substrate material for graphene.<sup>6,7</sup> Hexagonal boron nitride is a wide gap insulator that shares similar crystalline structure with graphene, but is slightly lattice-mismatched from it by about  $\sim 1.5\%$ . Micromechanically cleaved hBN layers can generally provide atomically smooth surfaces with fewer charge traps and dangling bonds than the commonly used  $\text{SiO}_2$  surfaces. Graphene layers on hBN have been shown to exhibit mobilities that are about an order of magnitude higher than those of graphene layers on  $\text{SiO}_2$ .<sup>6</sup> In addition, there are theoretical studies that show the interesting prospect of a spontaneous opening of a band gap in graphene due to the breaking of the A-B sublattice symmetry of graphene on hBN substrates.<sup>8</sup> Other studies have explored the tuning of band gaps in *single-layer* graphene on<sup>9</sup> and between<sup>10</sup> hBN sheets. Those studies use a different approach which leads to conclusions that are different from ours.

The objective of this paper is to report our investigations of the possibility of tuning band gaps in bilayer graphene (BLG) supported between hBN layers – a configuration of immediate practical relevance for electronic devices. Using density functional theory (DFT), we show that BLG essentially retains its freestanding properties<sup>11,12</sup> when it is “sandwiched” between hBN layers; furthermore, it shows a tunable band gap very much like its freestanding counterpart. The tunable band gap is relatively insensitive to the stacking order of BLG relative to hBN; this is not the case for a single-layer graphene on hBN. Indeed, Dean *et al.*<sup>6</sup> have noted the absence of a band gap in single-layer graphene on hBN. They attributed this to random stacking order, which might at best open up local gaps over short length scales. The relative insensitivity of BLG to stacking order, at least for the few cases considered here, suggests that BLG would be a suitable candidate for graphene-on-hBN

devices. We further consider the tunability of the band gap of single-layer graphene inserted between hBN layers and show, in contrast to previous work,<sup>10</sup> that single-layer graphene on hBN is a less suitable candidate for electronic device applications since it is *sensitive* to stacking and *insensitive* to applied external electric fields.

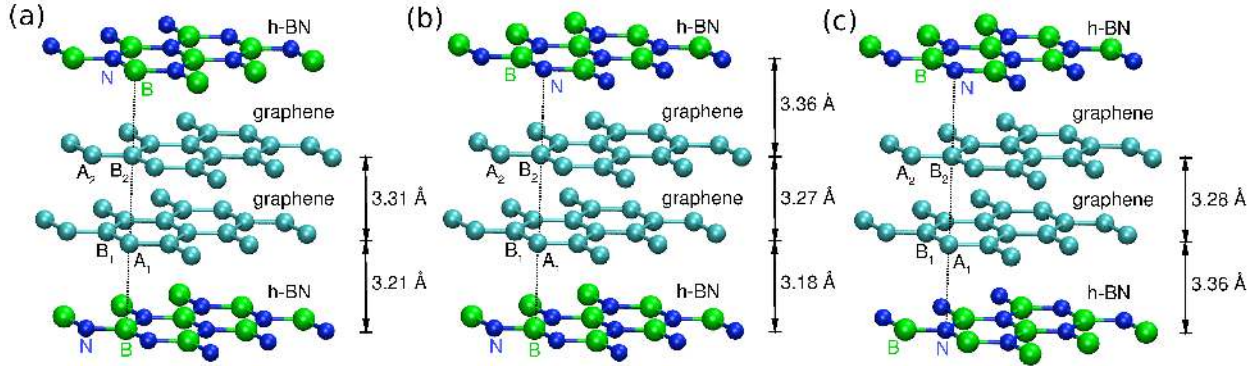


FIG. 1: Bilayer graphene between hBN layers. The layers have an overall Bernal (AB) stacking. Within this AB-stacking sequence the graphene and hBN layers can be arranged relative to each other to produce three different nearest-neighbor configurations along the  $c$ -axis, namely, (a) B-C-C-B, (b) B-C-C-N, and (c) N-C-C-N ordering. The A and B sublattices in both graphene layers are indicated in the figure. Equilibrium graphene-graphene and hBN-graphene spacings, as obtained from DFT calculations, are indicated in the figure.

The structure of BLG between two hBN layers (henceforth BLG/hBN) is schematically illustrated in Fig. 1. We envision that the hBN layers play the role of a substrate at the bottom and a top-gate dielectric for the BLG in between. The layers are arranged in a Bernal (AB) stacking order. In the model used for DFT simulations, the atomic positions and cell vectors are relaxed such that the forces on the atoms are less than  $0.01 \text{ eV}/\text{\AA}$  (see Methods for further details). For the stacking configurations illustrated in Figs. 1(a, c) where B or N atoms are directly below the C atom of the  $A_1$  sublattice and above the C atom of the  $B_2$  sublattice (forming B-C or B-N “dimers” in tight-binding parlance, which we adopt henceforth for convenience), there is no additional symmetry breaking arising from the relative disposition of the graphene and hBN layers. The dispersion of free-standing BLG is therefore unaltered by the presence of the substrate and one sees the usual touching of parabolic  $\pi$  and  $\pi^*$  bands at the  $K$ -point<sup>13</sup> [Fig. 2(b, c)]. For the stacking sequence of Fig. 1(b), in which there is a B atom below the C atom of the  $A_1$  sublattice, and an N

atom above the C atom of the B<sub>2</sub> sublattice, the hBN layers break the symmetry of the BLG by inducing a dipole across the layers; this opens up a small gap ( $\sim 40$  meV) at the  $K$  point [Fig. 2(d)]. Application of an external electric field normal to the basal planes of the structure renders the two graphene layers inequivalent, thus opening up a band gap in the vicinity of the  $K$  point while deforming the  $\pi$  ( $\pi^*$ ) bands such that the  $K$  point is now a local minimum (maximum) surrounded by two local maxima (minima). The true band gap of the structure is then no longer at the  $K$  point but rather along the  $\Gamma - K$  line of the Brillouin zone boundary.

The features described above can be seen in Fig. 2 where we illustrate the band structure of both freestanding BLG and BLG sandwiched between hBN. Figure 2 shows that the band structure of the BLG/hBN system is qualitatively identical to that of free-standing BLG. However, there are important quantitative differences in the actual values of band gaps. For clarity, the insets in Fig. 2 show the band gaps as functions of applied external electric fields. The insets show the true band gap ( $E_g$ ) and the  $\pi - \pi^*$  band openings at the  $K$  point ( $\Delta_K$ ) plotted as functions of the applied field. The latter varies linearly with the applied external field whereas the former tends to saturate with increasing electric field. Apparently, the hBN layers screen the BLG layers and suppress both the values of  $E_g$  and  $\Delta_K$ . This screening is especially evident at fields in the range of 0-2 V/nm for which the band gap for BLG/hBN system is only about half that of free-standing BLG. Eventually, both the band gap of the BLG/hBN system and that of free-standing BLG saturate at values of 0.22 eV and 0.28 eV, respectively. In theory, this saturation is not permanent as the nature of the gap actually changes from a direct value for the  $\pi$  and  $\pi^*$  bands near the  $K$ -point to an indirect one between the  $\pi$  band at  $K$  and the  $\pi^*$  band at  $\Gamma$ -point; the indirect gap progressively decreases with increasing electric field, leading eventually to a metallic state once the  $\pi^*$  band drops below the Fermi level at  $\Gamma$ . This semiconductor-metal transition is not particularly important as the fields required to reach it are sufficiently high that they would cause dielectric breakdown of the material before the transition is observed. For more practical fields in the range of 0-3 V/nm that are expected to be sustained by the BLG/hBN system, we conclude that the band gap is tunable over a range of  $\sim 0.2$  eV. The key point to note is that the dispersion of BLG is *not* fundamentally altered by the presence of the hBN layers nor is there any evidence of electron or hole doping as is common on metal surfaces (Ref. 15 and references within), SiC (Ref. 16 and references within) and Si/SiO<sub>2</sub>

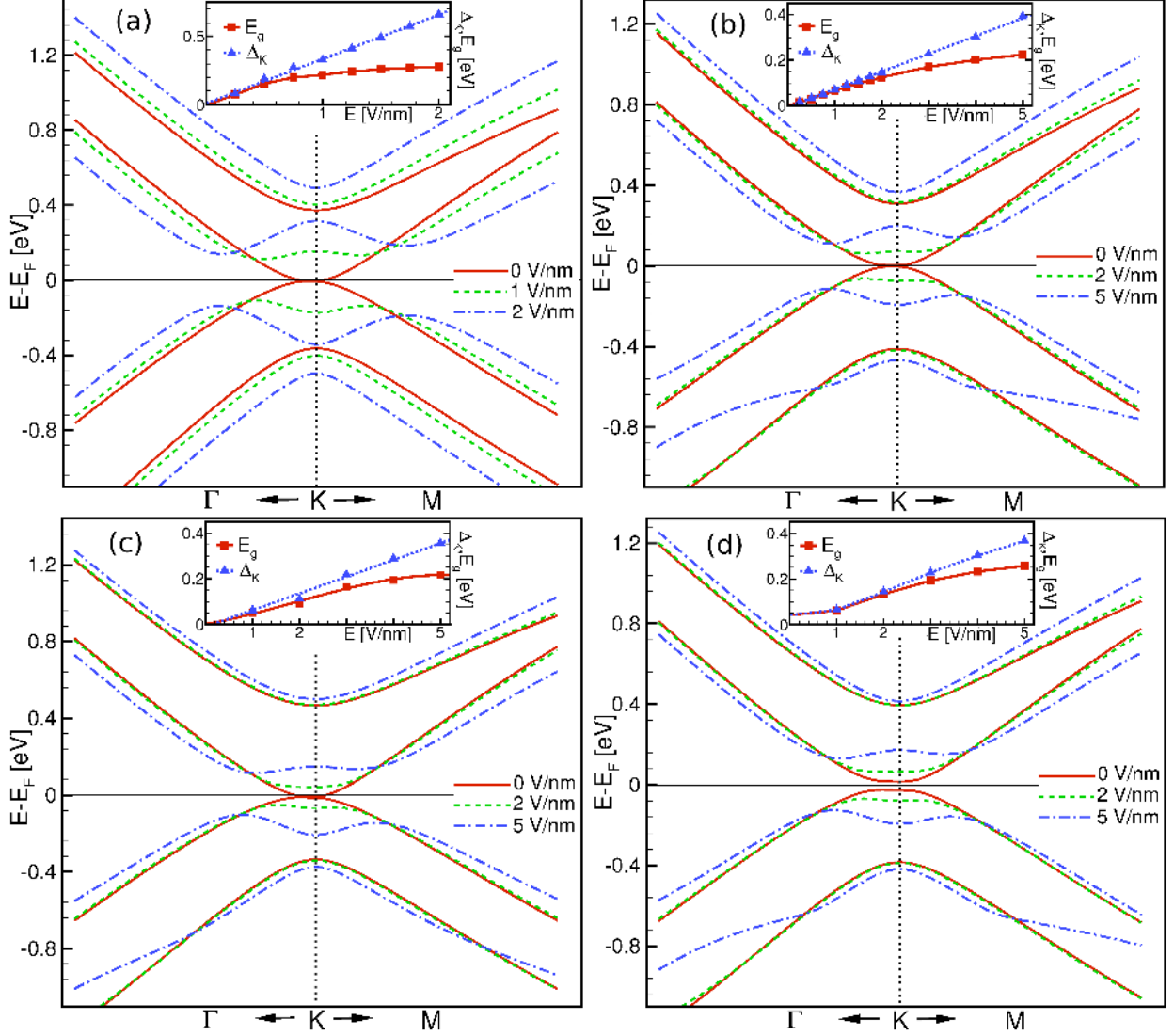


FIG. 2: Band structure in the vicinity of the  $K$  point as a function of external electric field for (a) BLG and for BLG/hBN with (b) B-C-C-B, (c) N-C-C-N, and (d) B-C-C-N ordering of dimers along the  $c$ -axis. Insets show band gaps ( $E_g$ ) and the gap at  $K$  ( $\Delta_K$ ) as a function of external field; the former saturates at higher values of  $E$  used here whereas the latter grows linearly. Here  $q$  varies up to value of 0.25 around  $K$ , *i.e.*,  $|K - q| \leq \pi/2a$ .

substrates.<sup>17</sup> These facts suggest that hBN could be a suitable substrate material for BLG in device applications.

One can obtain further insight into the influence of external fields on the electronic structure of BLG and the BLG/hBN system from Fig.3, which displays the atom projected

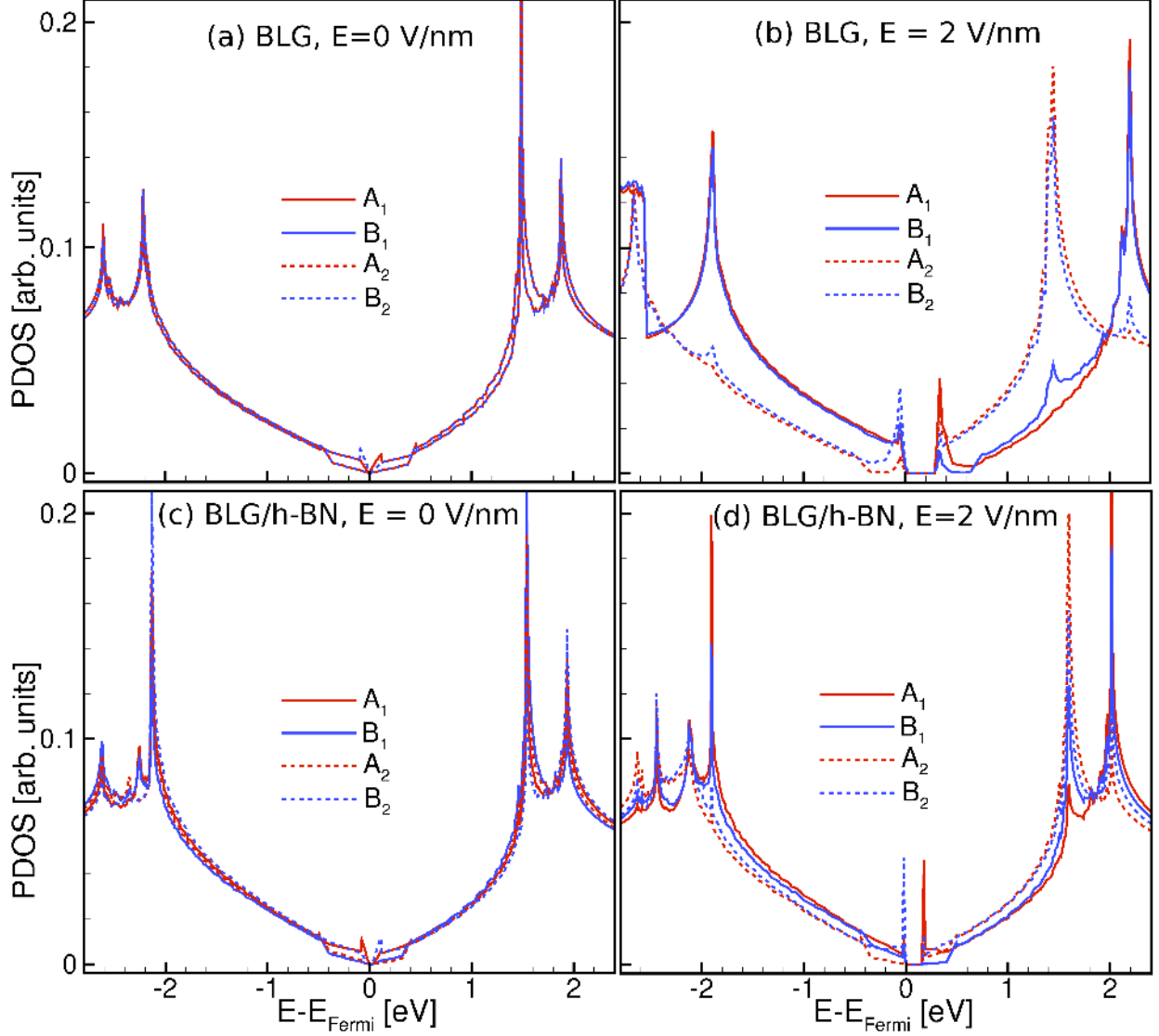


FIG. 3: Density of states arising from  $p_z$  orbitals projected on individual C atoms for BLG at external fields of (a) 0 V/nm and (b) 2 V/nm, and for BLG/hBN with B-C-C-B ordering of dimers along the  $c$ -axis at (c) 0 V/nm and (d) 2 V/nm. The remaining orbitals do not contribute significantly to states near the Fermi level, which are the only ones of importance here.

density of states derived from the  $p_z$  orbitals of the C atoms. These states are the only ones that contribute in the vicinity of the Fermi level and are important for understanding the electronic structure of BLG. Figures 3(a, c) show that there is some symmetry that is broken between the A and B sublattices of each individual graphene layer as expected for BLG, although there is no overall symmetry breaking between the two layers themselves. This

situation changes with the application of external electric fields as illustrated in Figs. 3(b, d), which show the asymmetric localization of valence and conduction states on each graphene layer, thereby rendering them inequivalent. The charge that is induced is mainly concentrated on the B sublattice of one layer (representing an occupied peak) whereas states at the conduction band edge localize on the A sublattice of the other layer.<sup>18</sup> For equivalent applied fields, symmetry breaking is more noticeable for BLG than the BLG/hBN system because the latter is screened by the hBN layers. The effect of the screening can be investigated by examining the distribution of the total local potential, which includes the usual nuclear, kinetic, Hartree, and exchange-correlation potentials, as well as the linear potential arising from the constant external electric field. In Fig. 4(a) we show the planar averaged local potential as a function of distance normal to the slab structure. The same information is displayed as the difference between the planar averaged local potential at finite field and that at zero field in Fig. 4(b) to clearly show the effect of the applied field. For BLG, we see that the local potential responds linearly to applied fields of up to 1.5 V/nm; for fields larger than 2 V/nm, there is some evidence of a nonlinear response in the vacuum region near the sheet surfaces. In spite of this, the internal screening within the graphene layers is sufficient to partially compensate the external field, allowing for an overall linear response of the BLG to external applied fields. This behavior justifies the treatment of BLG within the parallel plate capacitor approximation<sup>19,20</sup> for electric fields of this magnitude. For the BLG/hBN system, we note that the response of the local potential is still linear for fields as large as 5 V/nm. Interestingly, the difference in the planar averaged potential exhibits different slopes in the hBN-graphene and graphene-graphene regions due to different levels of internal screening within these regions [Fig. 4(b)]. Any significant nonlinearity is within the vacuum region and is an artifact attributed to proximity effects of the dipole used to apply the external field in the (VASP) program used for the simulations.<sup>21</sup> Overall, the hBN layers merely provide additional screening for the BLG; they do not fundamentally alter either the electronic properties of BLG or the tunability of its band gap.

For completeness, we examine the band structure of single-layer graphene inserted between hBN layers. It has been suggested by Sławińska *et al.*<sup>10</sup> that a single layer of graphene inserted between hBN layers in a rhombohedrally (ABC) stacked structure with nitrogen-carbon (N-C) dimers can exhibit a tunable gap as large as 0.23 eV. They further noted that other stacking configurations were less promising for tuning band gaps. We have



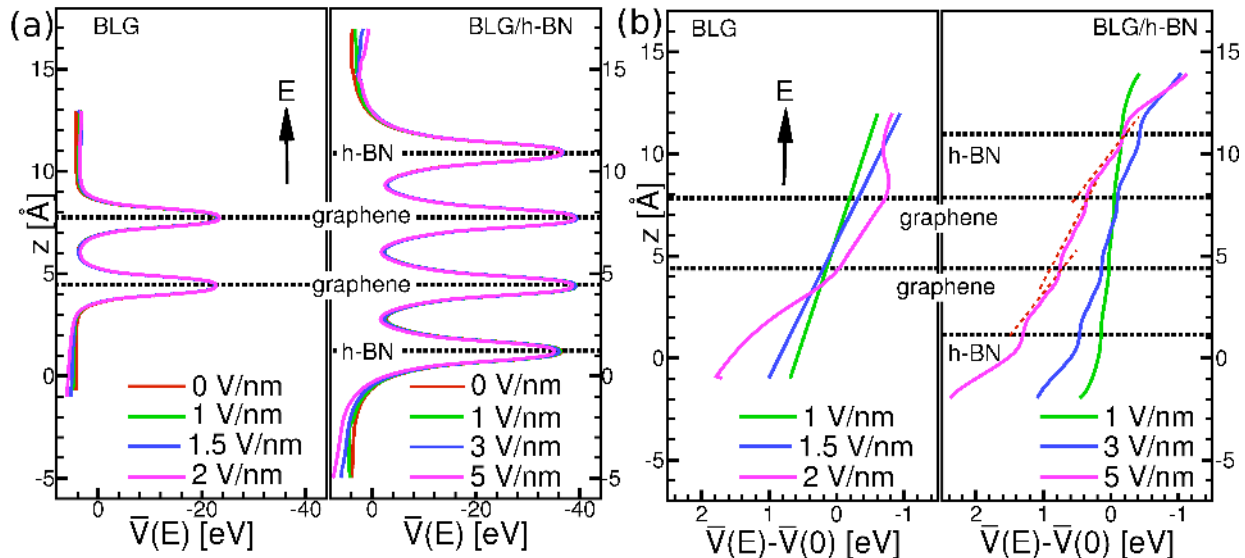


FIG. 4: (a) Local potential averaged over planes parallel to BLG and hBN sheets as a function of distance normal to the slab. (b) Difference between finite and zero-field planar averaged local potentials. Positions of the graphene and hBN planes are indicated in the figure. As seen, the hBN layers barely alter the linear variation in local potential with external fields across the graphene planes although they provide additional screening as evidenced from the steeper slope of the planar averaged potential difference curves for BLG/hBN compared to BLG. Also, note that the potential has a different slope between hBN and graphene and between the two graphene layers due to variations in internal screening within the structure. This is indicated by the red dotted line for the 5 V/nm case for BLG/hBN; similar variations occur for lower applied fields as well.

repeated these calculations for structures stacked in the Bernal and rhombohedral configurations for all possible combinations of C–B and C–N dimers; band structures in the vicinity of the  $K$  point are displayed Fig. 5 . Note that the usual linear dispersion characteristics of graphene are preserved at the  $K$  point, with the presence of a band gap even at zero external fields. The magnitude of the zero-field gap is sensitive to the stacking order and varies by about an order of magnitude (10 – 100 meV). However, for applied external fields as high as 5 V/nm, we find no evidence of significant changes in the zero-field band-gap—the gaps are either entirely non-tunable or, at best, slightly tunable. The difference between our results and those of Sławińska *et al.* is likely due to the fact that they used a tight-binding model with parameters fitted to DFT calculations; their model is probably unable to capture the

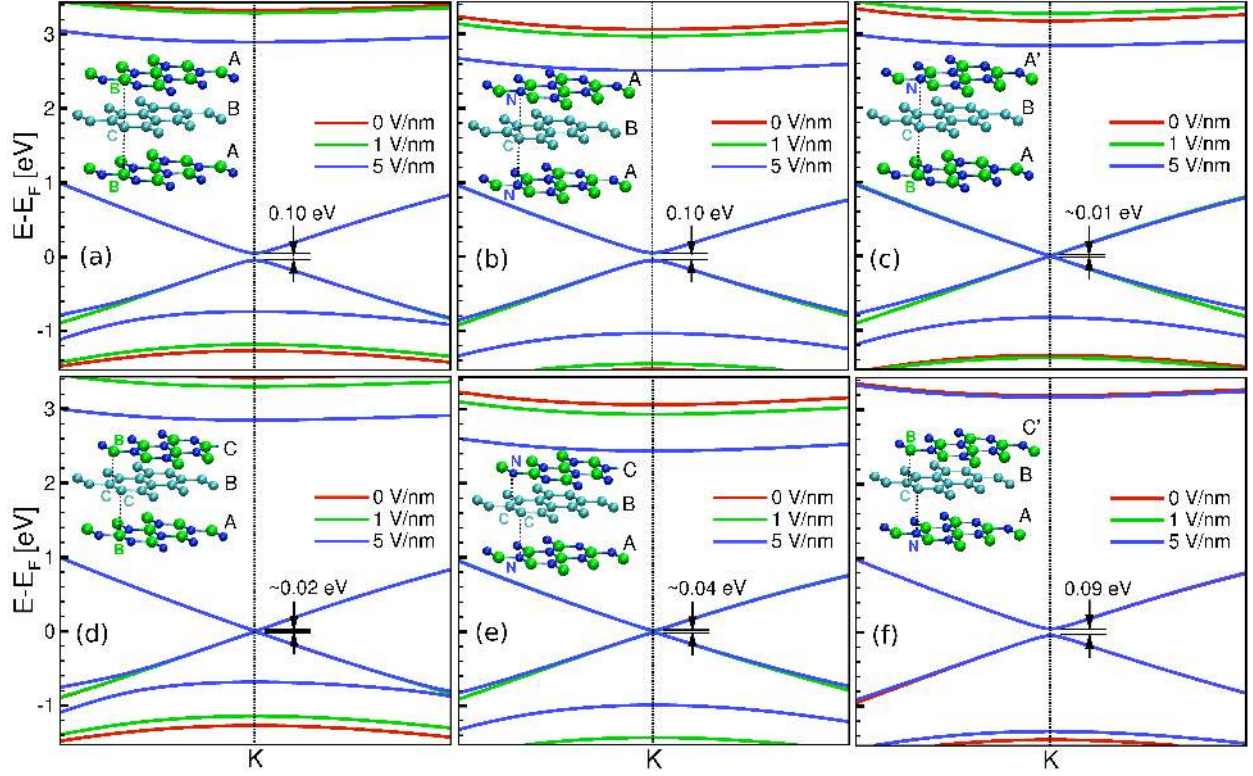


FIG. 5: Band structure in the vicinity of the  $K$  point as a function of external electric field for single layer graphene between hBN. Insets show atomic structures for various stackings as well as the B–C and N–C dimers. The upper row consists of Bernal (AB) stacked layers while the lower row consists of rhombohedral (ABC) stackings. As seen, the band gap is sensitive to both stacking sequence as well as the dimers formed along the  $c$ -axis, varying from near zero gaps to a maximum of 0.1 eV. However, the gap is not particularly sensitive to external electric fields.

physics of this system.<sup>26</sup> The largest possible gap that seems to be attainable in our calculations is about  $\sim 0.1$  eV ; this is not tunable, and is substrate-induced.<sup>8</sup> Interestingly, the induced bandgap roughly doubles when an SLG is sandwiched between two *in phase* BN layers compared to when the SLG is on a BN substrate. When the two BN layers are *out of phase* (translated or rotated), the bandgap decays to zero. In contrast to an SLG/hBN system, the BLG/hBN system exhibits a *continuously tunable* band gap of up to  $\sim 0.2$  eV and is *relatively robust* to stacking disorder (for the few configurations considered here).

In summary, we have investigated the electronic structure of BLG inserted between hBN layers using DFT calculations. We have examined the response of a BLG/hBN system to

external electric fields and shown that the structure exhibits a continuously tunable band gap of up to  $\sim 0.2$  eV. We note that in general, DFT calculations typically underestimate band gaps in materials; so it is conceivable that in practice larger band gaps than the ones reported in this work may be measured. By comparing our results for the BLG/hBN system to those obtained from free-standing BLG, we have shown that the hBN layers do not fundamentally alter the electronic properties of BLG, nor do they alter its response to electric fields, up to some screening effect. Moreover, our results indicate that the response of the BLG/hBN system is fairly robust to stacking disorder, which would be an important consideration for practical situations. In contrast, SLG/hBN structures are strongly sensitive to stacking configurations and are virtually insensitive to applied external electric fields. When considered in light of reported preliminary experiments, which show that hBN is a better substrate for graphene-based devices than  $\text{SiO}_2$ ,<sup>6</sup> our results suggest further promising avenues for the development of electronic devices based on the BLG/hBN system.

## Methods

DFT calculations were performed using the Vienna Ab Initio Simulation Package (VASP).<sup>22</sup> Core and valence electrons were described using the Projector-Augmented Wave method.<sup>23,24</sup> Electron exchange and correlation was treated using the Local Density Approximation as parameterized by Ceperley and Alder.<sup>25</sup> Atomic positions and cell vectors were relaxed using a conjugate gradient algorithm with a force tolerance of  $0.01$  eV/Å. Electronic minimization was performed with a tolerance of  $10^{-4}$  eV and electronic convergence was accelerated with a smearing of the Fermi surface by  $0.05$  eV. A Gaussian smearing was used during the relaxation procedure, followed by a Blöchl tetrahedron smearing for accurate density of states and local potential, and a Fermi smearing for non-self-consistent band-structure calculations. A  $75 \times 75 \times 1$  Monkhorst-Pack mesh was used for generating accurate charge densities, density of states, and local potentials. For BLG, SLG/hBN, and BLG/hBN, we used approximately  $11\text{Å}$ ,  $17\text{Å}$ , and  $20\text{Å}$  of vacuum between periodic images of the slabs. These values were chosen to ensure a smooth vacuum-level potential. We used a  $500$  eV kinetic energy cutoff for SLG and BLG/hBN. A larger cutoff for  $700$  eV was necessary for accurate DOS and local potentials for BLG/hBN due to more vacuum in the cell although a  $500$  eV cutoff was sufficient for band structures. Finally, electric fields were

applied normal to the slabs in VASP, which accomplishes this by introducing dipolar sheets at the center of the simulation cell.<sup>21</sup>

## Acknowledgments

A. Ramasubramaniam gratefully acknowledges new faculty startup funding from the University of Massachusetts. D. Naveh and E. Towe acknowledge the financial support of the Army Research Office and the National Science Foundation.

---

\* Electronic address: ashwin@engin.umass.edu

† Electronic address: naveh@cmu.edu

‡ Electronic address: towe@cmu.edu

- <sup>1</sup> Katsnelson, M. I.; Geim, A. K.; *Phil. Trans. R. Soc. A* **2007**, 366, 195.
- <sup>2</sup> Chen, J. H.; Jang, C.; Xiao, S.; Ishigami, M.; Fuhrer, M. S.; *Nature Nanotech.* **2008**, 3, 206.
- <sup>3</sup> Morozov, S. V.; Novoselov, K. S.; Katsnelson, M. I.; Schedin, F.; Elias, D. C.; Jaszczak, J. A.; Geim, A. K. *Phys. Rev. Lett.* **2008**, 016602 (100).
- <sup>4</sup> Zhang, Y.; Brar, V. W.; Girit, C.; Zettl, A.; Crommie, M. F. *Nature Physics* **2009**, 5, 722.
- <sup>5</sup> Fratini, S.; Guinea, F. *Phys. Rev. B* **2008**, 77, 195415.
- <sup>6</sup> Dean, C. R.; Young, A. F.; Meric, I.; Lee, C.; Wang, L.; Sorgenfrei, S.; Watanabe, K.; Taniguchi, T.; Kim, P.; Shepard, K. L.; Hone, J. *Nature Nanotech* **2010**, 5, 699.
- <sup>7</sup> Usachov, D.; Adamchuk, V. K.; Haberer, D.; Gr'üneis, A.; Sachdev, H.; Preobrajenski, A. B. *Phys. Rev. B* **2010**, 82, 075415.
- <sup>8</sup> Giovannetti, G.; Khomyakov, P. A.; Brocks, G.; Kelly, P. J.; van den Brink, J. *Phys. Rev.* **2006**, 76, 073103.
- <sup>9</sup> Śławińska, J.; Zasada, I.; Klusek, Z. *Phys. Rev. B* **2010**, 81, 155433.
- <sup>10</sup> Śławińska, J.; Zasada, I.; Kosiński, P.; Klusek, Z. *Phys. Rev. B* **2010**, 82, 085413.
- <sup>11</sup> Zhang, Y.; Tang, T.-T.; Girit, C.; Hao, Z.; Martin, M. C.; Zettl, A.; Crommie, M. F.; Shen, Y. R.; Wang, F. *Nature* **2009**, 459, 820823.
- <sup>12</sup> Ohta, T.; Bostwick, A.; Seyller, T.; Horn, K.; Rotenberg, E. *Science* **2006**, 313, 951954.

- <sup>13</sup> A. H. Castro Neto, F. Guinea, N. M. R. Peres, K. S. Novoselov, and A. K. Geim, *Rev. Mod. Phys.* **81**, 109 (2009).
- <sup>14</sup> Sutter, P.; Hybertson, M. S.; Sadowski, J. T.; Sutter, E. *Nano Letters* **2009**, 9, 3654.
- <sup>15</sup> Wintterlin, J.; Bocquet, M.-L. *Surface Sci.* **2009**, 603, 1841.
- <sup>16</sup> Riedl, C.; Coletti, C.; Starke, U. *J. Phys. D: Appl. Phys.* **2010**, 43, 374009.
- <sup>17</sup> Romero, H. E.; Shen, N.; Joshi, P.; Gutierrez, H. R.; Tadigadapa, S. A.; Sofo, J. O.; Eklund, P. C. *ACS Nano* **2008**, 2, 2037.
- <sup>18</sup> Yu, E. K.; Stewart, D. A.; Tiwari, S. *Phys. Rev. B* **2008**, 77, 195406.
- <sup>19</sup> Gava, P.; Lazzeri, M.; Saitta, A. M.; Mauri, F. *Phys. Rev. B* **2009**, 79, 165431.
- <sup>20</sup> Castro, E. V.; Novoselov, K. S.; Morozov, S. V.; Peres, N. M. R.; Lopes dos Santos, J. M. B.; Nilsson, J.; Guinea, F.; Geim, A. K.; Castro Neto, A. H. *J. Phys.: Condensed Matter* **2010**, 22, 175503 (2010).
- <sup>21</sup> Neugebauer, J.; Scheffler, M. *Phys. Rev. B* **1992**, 46, 6067.
- <sup>22</sup> Kresse, G.; Furthmüller, J. *Comput. Mat. Sci.* **1996**, 6, 15; *Phys. Rev. B* **1996** 54, 11169.
- <sup>23</sup> Blochl, P. E. *Phys. Rev. B* **1994**, 50, 17953.
- <sup>24</sup> Kresse, G.; Joubert, D.; *Phys. Rev. B* **1999**, 59, 1758.
- <sup>25</sup> Ceperley, D. M.; Alder, B. J. *Phys. Rev. Lett.* **1980**, 45, 566.
- <sup>26</sup> There is also a discrepancy between the DFT band structure in their work (Fig. 4 of Ref.10), which shows the unexpected presence of an energy level between the Dirac cones at the *K* point, and the band structures reported here.